ACSNANO
www.acsnano.org
ARTICLE

Fully Packaged Blue Energy Harvester by Hybridizing a Rolling Triboelectric Nanogenerator and an Electromagnetic Generator

Xin Wang,[†,‡,⊥] Zhen Wen,[†,§,⊥] Hengyu Guo,[†] Changsheng Wu,[†] Xu He,[†] Long Lin,[†] Xia Cao,[*,∥] and Zhong Lin Wang[*,†,∥]

[†]School of Materials Science and Engineering, Georgia Institute of Technology, Atlanta, Georgia 30332, United States

[‡]Suzhou Institute of Nano-Tech and Nano-Bionics, Chinese Academy of Sciences, Suzhou 215123, China

[§]Institute of Functional Nano and Soft Materials (FUNSOM), Jiangsu Key Laboratory for Carbon-Based Functional Materials and Devices, Soochow University, Suzhou 215123, China

[∥]Beijing Institute of Nanoenergy and Nanosystems, Chinese Academy of Sciences, Beijing 100083, China

Supporting Information

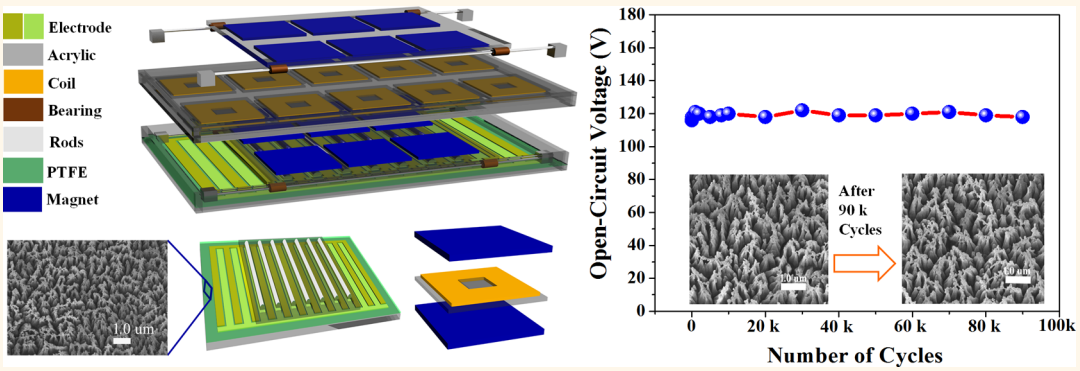

ABSTRACT: Ocean energy, in theory, is an enormous clean and renewable energy resource that can generate electric power much more than that required to power the entire globe without adding any pollution to the atmosphere. However, owing to a lack of effective technology, such blue energy is almost unexplored to meet the energy requirement of human society. In this work, a fully packaged hybrid nanogenerator consisting of a rolling triboelectric nanogenerator (R-TENG) and an electromagnetic generator (EMG) is developed to harvest water motion energy. The outstanding output performance of the R-TENG (45 cm^3 in volume and 28.3 g in weight) in the low-frequency range (<1.8 Hz) complements the ineffective output of EMG (337 cm^3 in volume and 311.8 g in weight) in the same range and thus enables the hybrid nanogenerator to deliver valuable outputs in a broad range of operation frequencies. Therefore, the hybrid nanogenerator can maximize the energy conversion efficiency and broaden the operating frequency simultaneously. In terms of charging capacitors, this hybrid nanogenerator provides not only high voltage and consistent charging from the TENG component but also fast charging speed from the EMG component. The practical application of the hybrid nanogenerator is also demonstrated to power light-emitting diodes by harvesting energy from stimulated tidal flow. The high robustness of the R-TENG is also validated based on the stable electrical output after continuous rolling motion. Therefore, the hybrid R-TENG and EMG device renders an effective and sustainable approach toward large-scale blue energy harvesting in a broad frequency range.

KEYWORDS: *blue energy harvester, rolling triboelectric nanogenerator, hybrid nanogenerator, water motion*

With rapidly increasing global energy consumption, growing research efforts have been devoted to exploit clean and renewable energy resources such as wind, ocean, and solar energies, *etc.* for sustainable

Received: October 1, 2016
Accepted: November 22, 2016
Published: November 22, 2016

DOI: 10.1021/acsnano.6b06622
ACS Nano XXXX, XXX, XXX−XXX

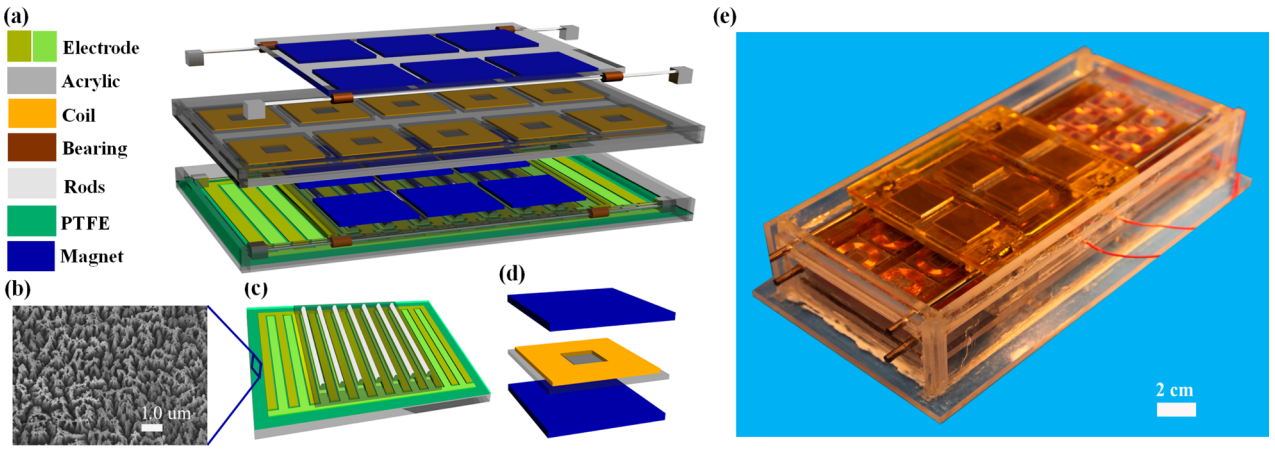

Figure 1. Structural design of blue energy hybrid nanogenerator. (a) Schematic illustration of the R-TENG and EMG. (b) SEM of nanowires on the PTFE thin film. (c) Schematic illustration of the TENG, which consists of a group of aluminum rods and PTFE thin film coated with the copper interdigitated electrodes. (d) Schematic illustration of the EMG unit, which consists of a pair of magnets and a coil. (e) Photograph of the TENG and EMG hybrid nanogenerator. The TENG is 45 cm^3 in volume and 28.3 g in weight. The EMG is 337 cm^3 in volume and 311.8 g in weight.

development of modern society.[1] Among them, blue energy, such as tidal energy, wave energy, current energy, osmosis, and so on, is of great advantage owing to the widely distributed water kinetic energy that is independent of weather, daylight, and seasonality.[2,3] However, large-scale harvesting of blue energy faces huge challenges because of high cost, engineering difficulties, seawater erosion of facilities, and very low efficiency.[4,5] The current main approach of using electromagnetic generators (EMGs) suffers from the low conversion efficiency due to the drastic decay in output power with the decrease of operating frequency (<5 Hz).[4,6]

Recently, triboelectric nanogenerators (TENGs), based on the coupling of triboelectrification and electrostatic induction, have been invented to harvest almost all forms of mechanical energies, such as vibrations, human walking, body motions, and even water waves.[7−26] TENGs have attracted strong research interest owing to high energy conversion efficiency, low cost, simply fabrication, light weight, and environmentally friendly processes.[5] In particular, the efficiency of the TENG is much higher than that of EMG in harvesting low-frequency mechanical energy.[6] This advantageous characteristics inspired some pioneering efforts in using TENGs to harvest wave energy, but their outputs are too low to be suitable for large-scale energy harvesting.[3,4,27,28] Recently, Guo *et al.*[29] and Wen *et al.*[30] have demonstrated a better model for harvesting blue energy by hybridizing a sliding-freestanding-mode TENG and an EMG. However, this sliding operation mode suffers from huge resistance in water and large wearing of the triboelectric surface. Therefore, to effectively harvest underwater low-frequency blue energy, an advanced structural design needs to be further optimized for practical application. One promising improvement is to replace a sliding-freestanding TENG with a rolling-freestanding TENG, which has been proven to be effective in reducing material abrasion and improving energy conversion efficiency.[31−34]

Herein, a strategy that hybridizes a rolling-freestanding triboelectric nanogenerator (R-TENG) with an EMG is proposed for harvesting blue energy. After a systematic comparison of the output performances of R-TENG with EMG, the results indicate that the R-TENG is more effective than EMG in collecting blue energy in the low-frequency range (<1.8 Hz). This complementary output performance enables the hybrid nanogenerator to deliver satisfactory outputs in a broad range of operation frequencies. Moreover, the capacitor charging characteristics show that this hybrid nanogenerator offers not only high voltage and consistent charging from the TENG component but also fast charging speed from the EMG component. The hybrid nanogenerator is also demonstrated to power light-emitting diodes (LEDs) by harvesting energy from stimulated tidal flow. This work renders an effective and sustainable approach toward large-scale blue energy harvesting in a broad frequency range.

RESULTS AND DISCUSSION

Device Structure. The basic unit of the hybrid nanogenerator consists of two parts: R-TENG and EMG, as schematically depicted in Figure 1a. The R-TENG is made of a group of rolling aluminum rods and polytetrafluoroethylene (PTFE) thin film coated with copper interdigitated electrodes (as shown in Figure 1c). To enhance surface charge density of contact electrification, ∼100 nm diameter, ∼1.0 μm long nanowires have been fabricated on the surface of PTFE thin film *via* inductively coupled plasma (ICP) etching, as shown in SEM of Figure 1b. The EMG part mainly consists of two sets of magnet groups (six pairs of square magnets) and a set of copper coils. Acrylic sheets of suitable sizes were used as structural support. The copper coils were sandwiched between the square magnets (a basic unit of EMG shown in Figure 1d), whose motion was guided by four steel rods (>260 mm in length). The motion of the top magnets would drive the movement of the bottom ones due to the attractive force between them, while the latter would further drive the rolling of aluminum rods due to the tight contact between the rods and the acrylic sheet onto which the bottom magnets were fixed. This is the key strategy to achieve the simultaneous operation of the R-TENG and EMG, and they can be fully isolated from the water environment by using the encapsulating acrylic sheets of suitable sizes. Figure 1e displays the photograph of the fully packaged R-TENG and EMG hybrid nanogenerator. The detailed fabrication process is described in the Experimental Section.

DOI: 10.1021/acsnano.6b06622
ACS Nano XXXX, XXX, XXX−XXX

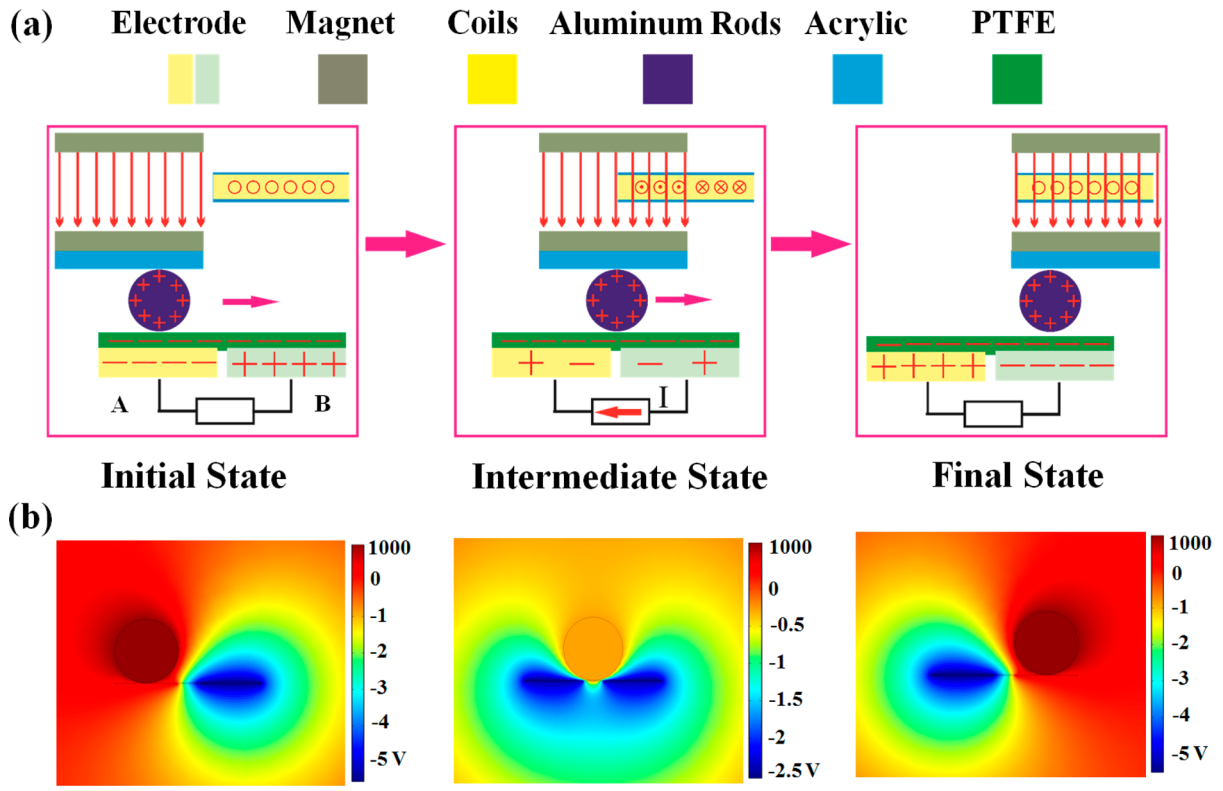

Figure 2. Schematic of the operation principle of the hybrid nanogenerator. (a) Scheme of the working mechanism of the TENG and EMG. (b) Numerical calculations of the potential distribution across the electrodes of the TENG under open-circuit condition at the three states, as evaluated by COMSOL.

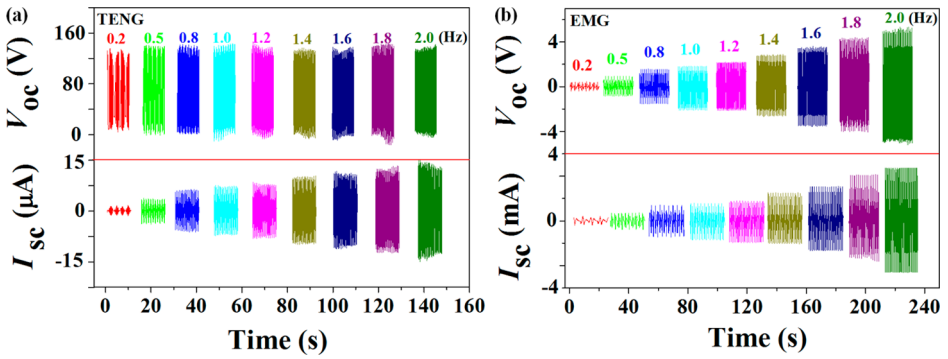

Figure 3. Electrical output performances. The open-circuit voltage (V_{oc}) and the short-circuit current (I_{sc}) of TENG (a) and EMG (b) under different operation frequency ranging from 0.2 to 2.0 Hz.

Working Principle. Figure 2a illustrates the detailed working principle of the hybrid nanogenerator, from which the electricity generation consists of two parts: one from R-TENG and the other from EMG. Herein, the working principle in a half circle was illustrated by current and charge distribution in short-circuit condition and magnetic flux for EMG. We define the initial state and final state as the states when the aluminum rod is aligned with electrode A and electrode B, respectively, which are a pair of interdigitated electrodes. The intermediate state represents the transitional process when the aluminum rod rolls between two electrodes. Similarly, the magnets in the initial and final states are fully misaligned and aligned with the copper coils, respectively. The operation of the device starts from the motion of the top magnet, accompanied by the movement of the bottom magnet and the aluminum rod. When permanent magnets of EMG move from the initial state to the final state, the magnetic flux crossing the copper coil will increase. According to the Lenz' s law, the increase of magnetic flux induces current in the coil to generate a new magnetic field to impede the increase of magnetic flux crossing the coil. Similarly, the transition between the final state and the next initial state induces the current flow in the reversed direction. Meanwhile, the aluminum rod with positive triboelectric charges will roll over the PTFE film with negative triboelectric charges from the initial state to the final state, introducing a potential drop and current flow between electrode A and electrode B *via* electrostatic induction. Specifically, when the rod moves from the initial state to the final state, the current would flow from B to A and *vice versa* when the rod continues to move from the final state to the next initial state.

To gain a more quantitative understanding of the proposed working principle of R-TENG, finite element analysis was

DOI: 10.1021/acsnano.6b06622
ACS Nano XXXX, XXX, XXX−XXX

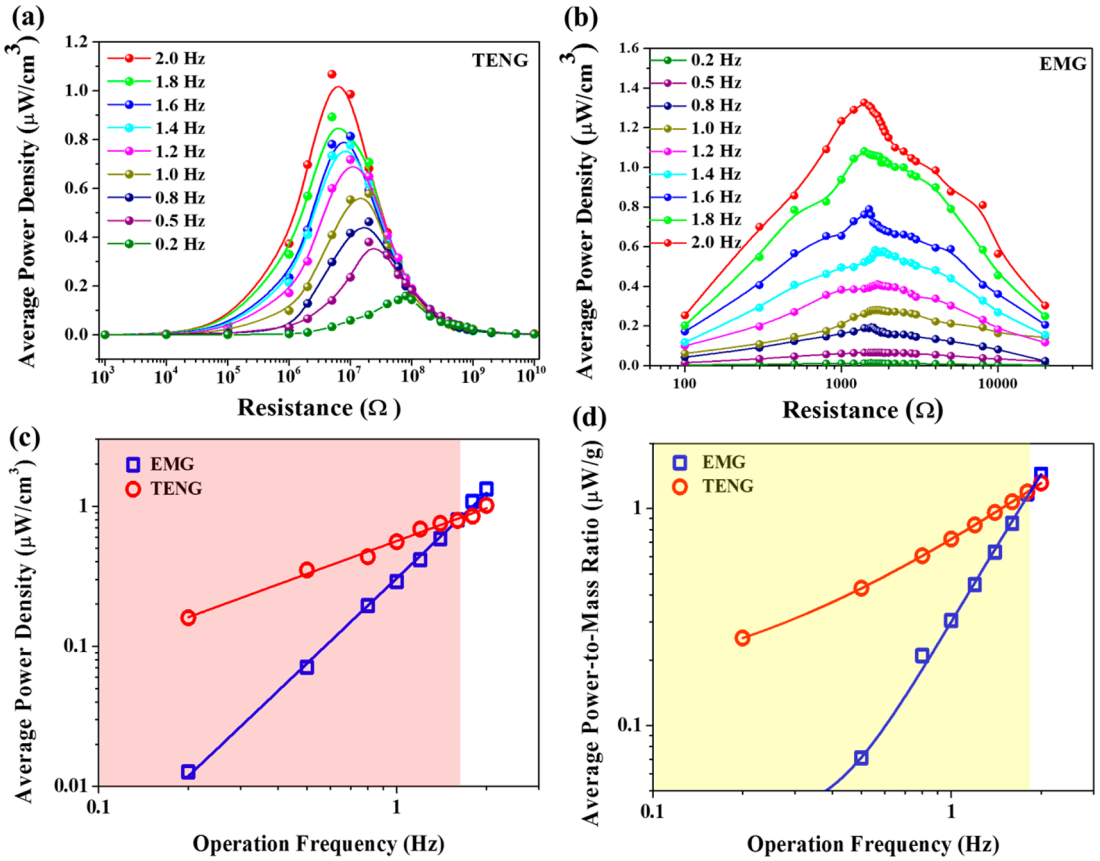

Figure 4. Output power performances of TENG and EMG. The dependence of the average power densities of TENG (a) and EMG (b) on the external load resistances. Average power densities (c) and average power-to-mass ratios (d) of TENG and EMG *versus* operation frequency (f) with linear fits of $\log_{10} P$ *vs* $\log_{10} f$. The fitted slopes for the TENG is about 1, while that for the EMG is about 2, which means that there is always an operation frequency range in which the output of TENG is larger than that of EMG, as marked by the pink and yellow areas, respectively.

employed to calculate open-circuit potential distribution across the interdigitated electrodes at the three different states with results displayed in Figure 2b. The calculated potential distribution across the two electrodes is consistent with the proposed working principles. In the initial state when the aluminum rod is aligned with the electrode A, the potential on electrode A is much higher than that on the electrode B and results in the maximum open-circuit voltage (V_{oc}). The V_{oc} decreases as the aluminum rod rolls from the initial state to the intermediate state, where the potential on A and B is equal. When the rod continues to move from the intermediate state to the final state, the potential difference further decreases to become negative and reaches the minimum when the rod is aligned with electrode B. Similarly, the distribution of magnetic lines was also simulated in the three states by COMSOL, as shown in Supporting Information (Figure S1).

Energy Output. The operation of the R-TENG and EMG hybrid nanogenerator under different frequency was simulated using a linear motion. Figure 3 presents the typical electrical performance including open-circuit voltage (V_{oc}) and short-circuit current (I_{sc}) of R-TENG and EMG at different operation frequencies, respectively. As shown in Figure 3a, the peak value of the V_{oc} for R-TENG is about 120 V and independent of the operation frequency, while the I_{sc} of R-TENG is proportional to the operation frequency, increasing linearly from ~1.28 to ~13.5 μA. Remarkably, the output peak density increases also proportionally with the increase of operation frequency. According to previous study,[6] the open-circuit voltage and the short-circuit current of TENGs can be expressed as

$$V_{oc}^{TENG} = \frac{Q_{sc}}{C(x)} \quad (1)$$

$$I_{sc}^{TENG} = \frac{dQ_{sc}}{dt} \quad (2)$$

where Q_{sc} is the short-circuit charge transfer amount and $C(x)$ is the capacitance between two electrodes at various displacement x. Since the maximum charge transfer amount (Q_{sc} max) is proportional to the triboelectric surface charge density (σ) and triboelectric surface area (s) and $C(x)$ is dependent on x instead of the time (t), the peak value of the open-circuit voltage is independent of the operation frequency. However, the I_{sc} is closely related to t and has been proven to be proportional to the frequency. Therefore, the measured V_{oc} and I_{sc} of R-TENG are consistent with the theoretical results. For EMG, both the V_{oc} and I_{sc} are proportional to the operation frequency and increase from ~0.4 to ~4.92 V and from ~0.2 to ~3.1 mA, respectively, as shown in Figure 3b. According to Faraday's law, the open-circuit voltage and the short-circuit current of EMGs can be expressed as[29]

$$V_{oc}^{EMG} = -N\frac{d\phi}{dt} \quad (3)$$

DOI: 10.1021/acsnano.6b06622
ACS Nano XXXX, XXX, XXX−XXX

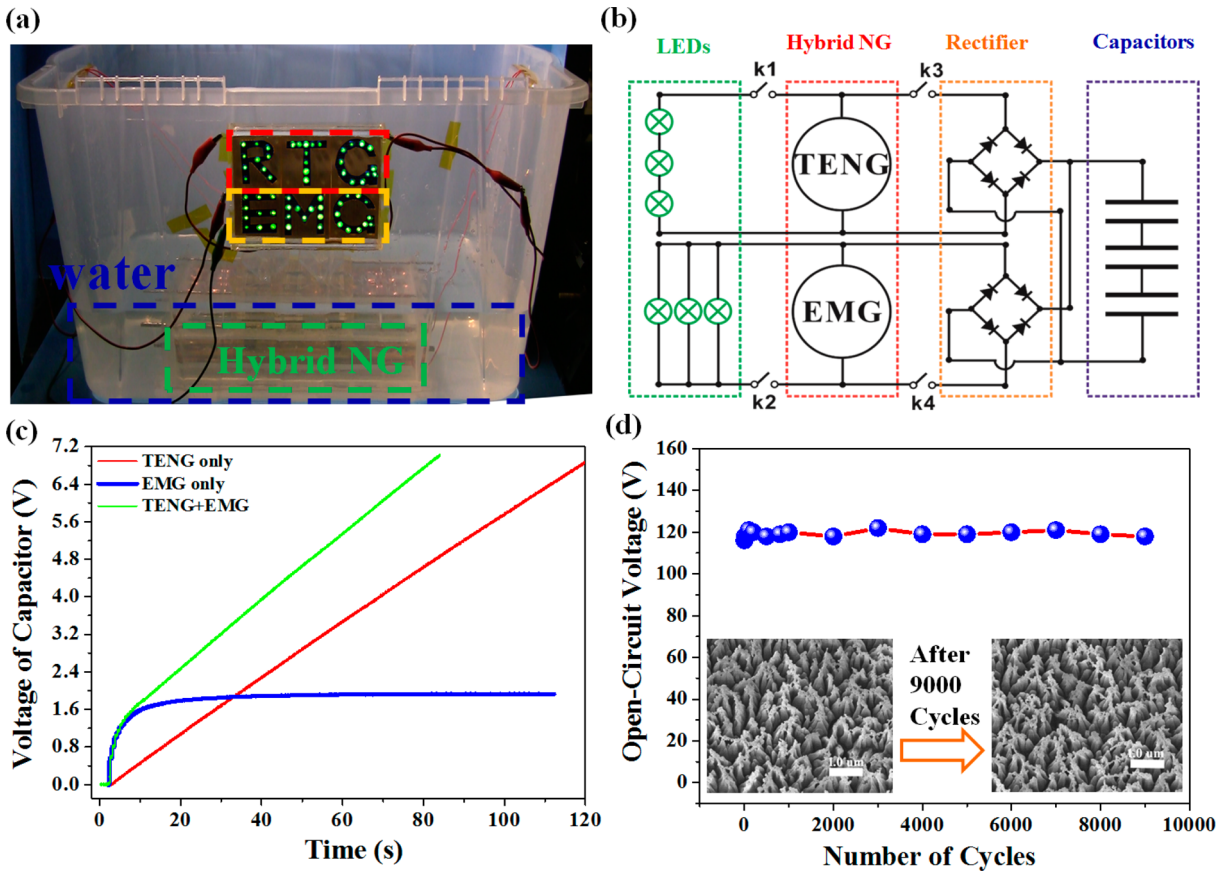

Figure 5. Demonstration of the packaged hybrid nanogenerator as a practical power source. (a) Photograph of the packaged hybrid nanognerator acting as the power source for lighting LEDs. The red rectangle frame displays 30 green LEDs in series comprising the "RTG" letters that are connected to the TENG. The yellow rectangle frame displays 30 green LEDs in parallel comprising the "EMG" letters that are connected to the EMG. The packaged hybrid nanogenerator was employed for lighting up the "RTG" and "EMG" LEDs under simulated ocean conditions. (b) Circuit diagram for lighting LEDs and charging capacitors. (c) Charging curves of a 20 μF capacitor using TENG only, EMG only, and hybrid nanogenerator, which shows that hybrid charging offers both the high charging voltage and the fast charging speed. (d) Robustness and stability investigation of the TENG. No obvious electrical output decay was observed after 9000 rolling cycles (at a fixed motion frequency of 1.0 Hz for 1 day). Inset: SEM images (scale bar is 1.0 μm) showing that no obvious distortion or serious damage was observed on the PTFE nanowire structure after continuous rolling.

$$I_{sc}^{EMG} = \frac{V_{oc}^{EMG}}{R} \quad (4)$$

where ϕ is the magnetic flux and N is the number of turns in the copper coils. R is the internal resistance of the coil. Based on eq 3, the output voltage of EMG is strongly related to the variation rate of the magnetic flux and the operation frequency. Therefore, the V_{oc} and I_{sc} of EMG should be proportional to the operation frequency, consistent with the experimental results.

To evaluate the energy output capability of the R-TENG and EMG, the average output power density of R-TENG and EMG when connected to different external load resistance was measured and calculated, as shown in Figure 4a,b, with a maximum value of 1.05 μW/cm^3 for R-TENG and 1.32 μW/cm^3 for EMG at corresponding matched load. The high output impedance of TENG can be lowered by a recently explored power-management system.[35] Furthermore, the correlation between the average power density (with respect to volume) and the operation frequency (f) was investigated for the R-TENG and EMG, respectively, as shown in Figure 4c. It can be found that the optimized average power density of R-TENG is proportional to the operation frequency (~0.15 to ~1.05 μW/cm^3), while that of EMG is proportional to the square of the operation frequency (~0.025 to ~1.32 μW/cm^3), consistent with previous work.[6] The output performance of R-TENG is better than that of EMG at an operation frequency less than 1.6 Hz, as marked by the pink area in Figure 4c. Considering that TENG has abundant choices of lightweight materials while EMG is mainly made of heavy magnets and metal coils, the optimized average power-to-mass ratio was also studied to incorporate the effects of material availability, as shown in Figure 4d. It turns out that the average power-to-mass ratio of the R-TENG is much better than that of EMG in an even larger-frequency range (about 1.8 Hz), as marked by the yellow area. Therefore, the R-TENG offers a more effective method than the EMG to harvest low-frequency energy.

Practical Demonstration. To explore the capability of the hybrid nanogenerator for large-scale blue energy harvesting, the full packaging strategy was employed to isolate the device from external water environment. For the experimental demonstration, a homemade water tank was applied to simulate real ocean environment. One group of green LEDs is connected to the R-TENG in series, assembling the word "RTG". Another group of green LEDs, constituting the word "EMG", is connected to the EMG in parallel. It was observed that the packaged R-TENG

DOI: 10.1021/acsnano.6b06622
ACS Nano XXXX, XXX, XXX−XXX

could work and generate stable electrical output when the device was immerged into water, as shown in Movie S1. The observed lighting of LEDs indicates the packaging works as an effective waterproof method to protect the TENG electrodes from being short-circuited. Additionally, the packaged hybrid nanogenerator was also utilized for lighting the "RTG" and "EMG" LEDs directly under simulated tide flow, as seen in Figure 5a and Movie S2. Furthermore, the output of the hybrid nanogenerator was also demonstrated to charge a 20 μF capacitor through a rectifier. The circuit diagram of lighting LEDs and charging capacitor by the hybrid nanogenerator is illustrated in Figure 5b. The charging voltage curves of the capacitor using R-TENG only, EMG only, and hybrid nanogenerator are plotted in Figure 5c and Figure S2, which suggests that the charging characteristic heavily depends on the inherent output performance of R-TENG and EMG. Specially, the output voltage determines the final charging level, while the output current determines the charging speed. Due to the high output voltage and low output current of R-TENG, the voltage of the capacitor charged by R-TENG can be charged up to the maximum open-circuit voltage (10−120 V) with a long charging time. In contrast, the voltage of the capacitors charged by EMG is limited by the low open-circuit voltage of EMG (usually less than ∼3 V) and quickly saturated within short charging time, leading to great loss of the energy harvested. The hybrid charging (TENG + EMG) provides not only high charging voltage but also fast charging speed. Moreover, the rate of charging a capacitor using a TENG can also be greatly enhanced through the reported power-management system[35] and the designed charging cycle.[36] To demonstrate the advantage and reliability of R-TENG, the device robustness has been examined by the stability of the electrical output and mechanical durability. Figure 5d shows that less than ±3% of electrical output fluctuation was observed after continuous operation of 9000 cycles (with a fixed rolling frequency of 1 Hz for 1 day). Meanwhile, the nanowire morphologies of the PTFE film surface exhibited no significant distortion or serious damage after continuous rolling of 9000 cycles, as shown in the inset of Figure 5d. This validates the mechanical durability of the R-TENG and can be attributed to the reduced friction from rolling compared to sliding. The outstanding robustness of the R-TENG enables long-term stability under harsh water environment, which is considered an important improvement of hybrid nanogenerator as a blue energy harvester.

CONCLUSION

In summary, we have demonstrated a fully packaged R-TENG and EMG hybrid nanogenerator that can be used for harvesting blue energy from ocean tides and currents. In this design, the R-TENG is indirectly driven by the noncontact attractive forces between pairs of magnets thus can be easily hybridized with the EMG. Furthermore, the fully packaged R-TENG and EMG hybrid nanogenerator could be completely isolated from external environment and work properly under water. Given that the R-TENG is more suitable for harvesting low-frequency energy, while the EMG generates larger output in the high-frequency range, hybridizing R-TENG with EMG enables the effective harvesting of blue energy with a broad frequency range. Finally, the packaged R-TENG and EMG hybrid nanogenerator was demonstrated to harvest simulated tidal flow energy to drive LEDs directly and a commercial charge capacitor. In terms of capacitor charging, the R-TENG and EMG hybrid nanogenerator offers not only high voltage charging but also rapid charging in the early period. The robustness and stability of the R-TENG were validated by the negligible degradation of electrical output after continuous rolling of more than 9000 cycles. Therefore, the packaged R-TENG and EMG hybrid nanogenerator provides an effective strategy for harvesting broad-frequency blue energy.

EXPERIMENTAL SECTION

Fabrication of the R-TENG. First, a mask based on polyvinyl-chloride film was processed by laser cutting (PLS6.75, Universal Laser Systems). Then the mask was attached on one rectangular 3.175 mm acrylic sheet (260 mm × 110 mm) as supporting substrate for the deposition of copper interdigitated electrodes using pulsed vapor deposition. Two electrical leads were connected to the two sets of interdigitated electrodes for electric measurement. The PTFE thin film with nanostructures was fabricated by using a common method reported previously.[14] The surface morphology of the PTFE thin film was characterized by field emission scanning electron microscopy (SEM) (Hitachi SU-8010). The as-prepared PTFE thin film was pasted to the top of interdigitated electrodes as the triboelectric layer. The PTFE film was covered by 10 aluminum rods (6.35 mm in diameter, 100 mm in length) that were polished with fine grit sandpaper to ensure a smooth working surface. The distance between any two aluminum rods matches that of a pair of interdigitated electrodes. The fabricated R-TENG is 45 cm^3 in volume and 28.3 g in weight.

Fabrication of EMG. For fabrication of EMG, two 1.5 mm acrylic sheets (130 mm × 110 mm) and six pairs of copper coils were first prepared. Both acrylic substrates have four grooves of 2 mm deep for fixing the sliding bearing at the corners. Then three pairs of NdFeB square permanent magnets (1.0 in. × 1.0 in. × 0.1 in.) with the same side of magnetic pole were arranged on the same side of one acrylic sheet and aligned to the magnets on the another acrylic sheet, and six pairs of copper coils (500 turns for each) were embedded in the 1.5 mm acrylic substrate with a physical gap between. Finally, the motion of the magnets would move with low friction under the assistance of linear ball bearings along two pairs of steel rods as support. The fabricated EMG is 337 cm^3 in volume and 311.8 g in weight.

Assembling of the Blue Energy Generator. Two 3.17 mm acrylic sheets (width × height: 120 mm × 65 mm) with three grooves and four holes were employed as support of the generator. The part attached to TENG was first fixed and then used to assemble the EMG. The acrylic sheet with down-magnets contacted tightly with the aluminum rods to enable their rolling by following the linearly motion of the NdFeB permanent magnets. Several encapsulation acrylic sheets with suitable sizes were utilized to form the waterproof wall to package simultaneously R-TENG and EMG except for the upper-magnets of EMG part. The packaged blue energy nanogenerator can be fully isolated from the external environment.

Electrical Measurement. The open-circuit voltage and short-circuit current of the devices were measured by a Keithley 6514 system electrometer. The software platform is constructed using LabVIEW and is capable of realizing real-time data collection and analysis.

Calculation of the Optimized Average Power Output.[6] When the R-TENG and EMG were connected to different external load resistance, the voltage across the resistance and the current flowing through the resistance were measured simultaneously. The schematic circuit is shown in Figure S3. Then the average output power was calculated using the following equation (t_0 is a randomly picked time during operations)

$$\overline{P^{\mathrm{TENG}}} = \frac{\int_{to}^{to+T} VI\,dt}{T} \tag{5}$$

Finally, the maximum power for each frequency was used to calculate the optimized average power density and average power-to-mass ratio, and the resistance corresponding to the maximum power is the matched load resistance.

DOI: 10.1021/acsnano.6b06622
ACS Nano XXXX, XXX, XXX−XXX

ASSOCIATED CONTENT

Supporting Information

The Supporting Information is available free of charge on the ACS Publications website at DOI: 10.1021/acsnano.6b06622.

Distribution of magnetic lines in the three states calculated by the COMSOL (Figure S1); voltage of a 20 μF capacitor charged by TENG and EMG under different operation frequency (Figure S2); and schematic circuit diagram for output power measurement (Figure S3) (PDF)

Movie S1: Electric output performance of the packaged R-TENG under water environment (AVI)

Movie S2: Packaged R-TENG and EMG hybrid nanogenerator for harvesting blue energy (AVI)

AUTHOR INFORMATION

Corresponding Authors

*E-mail: caoxia@binn.cas.cn.

*E-mail: zhong.wang@mse.gatech.edu.

ORCID

Zhong Lin Wang: 0000-0002-5530-0380

Author Contributions

⊥X.W. and Z.W. contributed equally to this work.

Notes

The authors declare no competing financial interest.

ACKNOWLEDGMENTS

This research was supported by the Hightower Chair Foundation and the "Thousands Talents" program for Pioneer Researcher and His Innovation Team, China, National Natural Science Foundation of China (Grant Nos. 5151101243, 51561145021, 11174324, and 10804082), the National Key R&D Project from Minister of Science and Technology (2016YFA0202704) and the Youth Innovation Promotion Association of CAS (Grant No. 2011235). The authors would like to express our sincere gratitude to the China Scholarship Council (CSC) and Chinese Academy of Sciences (CAS) for the scholarship to support their study in the Georgia Institute of Technology, United States.

REFERENCES

(1) Tollefson, J. Power from the Oceans: Blue Energy. *Nature* **2014**, *508*, 302−304.

(2) Falcao, A. F. O. Wave Energy Utilization: A Review of the Technologies. *Renewable Sustainable Energy Rev.* **2010**, *14*, 899−918.

(3) Chen, J.; Yang, J.; Li, Z.; Fan, X.; Zi, Y.; Jing, Q.; Guo, H.; Wen, Z.; Pradel, K. C.; Niu, S.; Wang, Z. L. Networks of Triboelectric Nanogenerators for Harvesting Water Wave Energy: A Potential Approach toward Blue Energy. *ACS Nano* **2015**, *9*, 3324−3331.

(4) Jiang, T.; Zhang, L. M.; Chen, X.; Han, C. B.; Tang, W.; Zhang, C.; Xu, L.; Wang, Z. L. Structural Optimization of Triboelectric Nanogenerator for Harvesting Water Wave Energy. *ACS Nano* **2015**, *9*, 12562−12572.

(5) Khan, U.; Kim, S. W. Triboelectric Nanogenerators for Blue Energy Harvesting. *ACS Nano* **2016**, *10*, 6429−6432.

(6) Zi, Y.; Guo, H.; Wen, Z.; Yeh, M. H.; Hu, C.; Wang, Z. L. Harvesting Low-Frequency (< 5 Hz) Irregular Mechanical Energy: A Possible Killer Application of Triboelectric Nanogenerator. *ACS Nano* **2016**, *10*, 4797−4805.

(7) Wang, Z. L. Triboelectric Nanogenerators as New Energy Technology and Self-Powered Sensors - Principles, Problems and Perspectives. *Faraday Discuss.* **2014**, *176*, 447−458.

(8) Wang, Z. L.; Chen, J.; Lin, L. Progress in Triboelectric Nanogenerators as A New Energy Technology and Self-Powered Sensors. *Energy Environ. Sci.* **2015**, *8*, 2250−2282.

(9) Wu, C.; Wang, X.; Lin, L.; Guo, H.; Wang, Z. L. Paper-Based Triboelectric Nanogenerators Made of Stretchable Interlocking Kirigami Patterns. *ACS Nano* **2016**, *10*, 4652−4659.

(10) Xie, Y.; Wang, S.; Niu, S.; Lin, L.; Jing, Q.; Yang, J.; Wu, Z.; Wang, Z. L. Grating-Structured Freestanding Triboelectric-Layer Nanogenerator for Harvesting Mechanical Energy at 85% Total Conversion Efficiency. *Adv. Mater.* **2014**, *26*, 6599−6607.

(11) Zhu, G.; Su, Y.; Bai, P.; Chen, J.; Jing, Q.; Yang, W.; Wang, Z. L. Harvesting Water Wave Energy by Asymmetric Screening of Electrostatic Charges on A Nanostructured Hydrophobic Thin-Film Surface. *ACS Nano* **2014**, *8*, 6031−6037.

(12) Wen, X.; Yang, W.; Jing, Q.; Wang, Z. L. Harvesting Broadband Kinetic Impact Energy from Mechanical Triggering/Vibration and Water Waves. *ACS Nano* **2014**, *8*, 7405−7412.

(13) Hu, Y.; Yang, J.; Jing, Q.; Niu, S.; Wu, W.; Wang, Z. L. Triboelectric Nanogenerator Built on Suspended 3D Spiral Structure as Vibration and Positioning Sensor and Wave Energy Harvester. *ACS Nano* **2013**, *7*, 10424−10432.

(14) Zhu, G.; Zhou, Y.; Bai, P.; Meng, X.; Jing, Q.; Chen, J.; Wang, Z. L. A Shape-Adaptive Thin-Film-Based Approach for 50% High-Efficiency Energy Generation Through Micro-Grating Sliding Electrification. *Adv. Mater.* **2014**, *26*, 3788−3796.

(15) Yao, Y.; Jiang, T.; Zhang, L.; Chen, X.; Gao, Z.; Wang, Z. L. Charging System Optimization of Triboelectric Nanogenerator for Water Wave Energy Harvesting and Storage. *ACS Appl. Mater. Interfaces* **2016**, *8*, 21398−21406.

(16) Cheng, X.; Meng, B.; Zhang, X.; Han, M.; Su, Z.; Zhang, H. Wearable Electrode-Free Triboelectric Generator for Harvesting Biomechanical Energy. *Nano Energy* **2015**, *12*, 19−25.

(17) Bae, J.; Lee, J.; Kim, S.; Ha, J.; Lee, B. S.; Park, Y.; Choong, C.; Kim, J. B.; Wang, Z. L.; Kim, H. Y.; Park, J. J.; Chung, U. I. Flutter-Driven Triboelectrification for Harvesting Wind Energy. *Nat. Commun.* **2014**, *5*, 4929.

(18) Wu, C.; Kim, T. W.; Li, F.; Guo, T. Wearable Electricity Generators Fabricated Utilizing Transparent Electronic Textiles Based on Polyester/Ag Nanowires/Graphene Core-Shell Nanocomposites. *ACS Nano* **2016**, *10*, 6449−6457.

(19) Huang, L.; Bai, G.; Wong, M.; Yang, Z.; Xu, W.; Hao, J. Magnetic-Assisted Noncontact Triboelectric Nanogenerator Converting Mechanical Energy into Electricity and Light Emissions. *Adv. Mater.* **2016**, *28*, 2744−2751.

(20) He, X.; Guo, H.; Yue, X.; Gao, J.; Xi, Y.; Hu, C. Improving Energy Conversion Efficiency for Triboelectric Nanogenerator with Capacitor Structure by Maximizing Surface Charge Density. *Nanoscale* **2015**, *7*, 1896−1903.

(21) Ha, M.; Park, J.; Lee, Y.; Ko, H. Triboelectric Generators and Sensors for Self-Powered Wearable Electronics. *ACS Nano* **2015**, *9*, 3421−3427.

(22) Chen, L.; Guo, H.; Xia, X.; Liu, G.; Shi, H.; Wang, M.; Xi, Y.; Hu, C. Novel Spiral-Like Electrode Structure Design for Realization of Two Modes of Energy Harvesting. *ACS Appl. Mater. Interfaces* **2015**, *7*, 16450−16457.

(23) Lee, J. H.; Hinchet, R.; Kim, T. Y.; Ryu, H.; Seung, W.; Yoon, H. J.; Kim, S. W. Control of Skin Potential by Triboelectrification with Ferroelectric Polymers. *Adv. Mater.* **2015**, *27*, 5553−5558.

(24) Kwak, S. S.; Lin, S.; Lee, J. H.; Ryu, H.; Kim, T. Y.; Zhong, H.; Chen, H.; Kim, S. W. Triboelectrification-Induced Large Electric Power Generation from A Single Moving Droplet on Graphene/Polytetrafluoroethylene. *ACS Nano* **2016**, *10*, 7297−7302.

(25) Liu, G.; Liu, R.; Guo, H.; Xi, Y.; Wei, D.; Hu, C. A Novel Triboelectric Generator Based on the Combination of A Waterwheel-Like Electrode with a Spring Steel Plate For Efficient Harvesting of Low-Velocity Rotational Motion Energy. *Adv. Electron. Mater.* **2016**, *2*, 1500448.

(26) Jin, Y.; Seo, J.; Lee, J. S.; Shin, S.; Park, H. J.; Min, S.; Cheong, E.; Lee, T.; Cho, S. W. Triboelectric Nanogenerator Accelerates

DOI: 10.1021/acsnano.6b06622
ACS Nano XXXX, XXX, XXX−XXX

Highly Efficient Nonviral Direct Conversion and In Vivo Reprogramming of Fibroblasts to Functional Neuronal Cells. *Adv. Mater.* **2016**, *28*, 7365−7374.
(27) Wang, X.; Niu, S.; Yin, Y.; Yi, F.; You, Z.; Wang, Z. L. Triboelectric Nanogenerator Based on Fully Enclosed Rolling Spherical Structure for Harvesting Low-Frequency Water Wave Energy. *Adv. Energy Mater.* **2015**, *5*, 1501467.
(28) Yang, Y.; Zhang, H.; Liu, R.; Wen, X.; Hou, T.; Wang, Z. L. Fully Enclosed Triboelectric Nanogenerators for Applications in Water and Harsh Environments. *Adv. Energy Mater.* **2013**, *3*, 1563−1568.
(29) Guo, H.; Wen, Z.; Zi, Y.; Yeh, M. H.; Wang, J.; Zhu, L.; Hu, C.; Wang, Z. L. A Water-Proof Triboelectric-Electromagnetic Hybrid Generator for Energy Harvesting in Harsh Environments. *Adv. Energy Mater.* **2016**, *6*, 1501593.
(30) Wen, Z.; Guo, H.; Zi, Y.; Yeh, M. H.; Wang, X.; Deng, J.; Wang, J.; Li, S.; Hu, C.; Zhu, L.; Wang, Z. L. Harvesting Broad Frequency Band Blue Energy by A Triboelectric-Electromagnetic Hybrid Nanogenerator. *ACS Nano* **2016**, *10*, 6526−6534.
(31) Lin, L.; Xie, Y.; Niu, S.; Wang, S.; Yang, P. K.; Wang, Z. L. Robust Triboelectric Nanogenerator Based on Rolling Electrification and Electrostatic Induction at an Instantaneous Energy Conversion Efficiency of similar to 55%. *ACS Nano* **2015**, *9*, 922−930.
(32) Lin, Z.; Cheng, G.; Li, X.; Yang, P.; Wen, X.; Wang, Z. L. A Multi-Layered Interdigitative-Electrodes-Based Triboelectric Nanogenerator for Harvesting Hydropower. *Nano Energy* **2015**, *15*, 256−265.
(33) Hu, Y.; Yang, J.; Niu, S.; Wu, W.; Wang, Z. L. Hybridizing Triboelectrification and Electromagnetic Induction Effects for High-Efficient Mechanical Energy Harvesting. *ACS Nano* **2014**, *8*, 7442−7450.
(34) Zhang, K.; Wang, X.; Yang, Y.; Wang, Z. L. Hybridized Electromagnetic-Triboelectric Nanogenerator for Scavenging Biomechanical Energy for Sustainably Powering Wearable Electronics. *ACS Nano* **2015**, *9*, 3521−3529.
(35) Niu, S.; Wang, X.; Yi, F.; Zhou, Y.; Wang, Z. L. A Universal Self-Charging System Driven by Random Biomechanical Energy for Sustainable Operation of Mobile Electronics. *Nat. Commun.* **2015**, *6*, 8975.
(36) Zi, Y.; Wang, J.; Wang, S.; Li, S.; Wen, Z.; Guo, H.; Wang, Z. L. Effective Energy Storage from A Triboelectric Nanogenerator. *Nat. Commun.* **2016**, *7*, 10987.

DOI: 10.1021/acsnano.6b06622
ACS Nano XXXX, XXX, XXX−XXX